Enhanced performance of InP/InGaAs HBT Phototransistor with an improved Base contact design

J. Thuret, C. Gonzalez, M. Riet and J.L. Benchimol
France Telecom/CNET/DTD/CBO, 196, avenue Henri Ravera, B.P. 107, 92225 Bagneux, FRANCE
julien.thuret@cnet.francetelecom.fr, carmen.gonzalez@cnet.francetelecom.fr, muriel.riet@cnet.francetelecom.fr, jeanlouis.benchimol@cnet.francetelecom.fr

Abstract

We report the electrical and photoresponse characteristics of InP/InGaAs HBT phototransistor (HPT) according to the base contact configuration. It is shown that improved base contact design can provide optical gain G_{opt} and unit optical gain cut-off frequency f_c very near to the current gain H_{21} and unit current gain cut-off frequency f_t of the phototransistor H_{21} and f_t being the upper limit performances of the HPT. f_c = 42 GHz for f_t = 55 GHz,(i.e. a f_c/f_t ratio = 0.76) were obtained for the type-B phototransistor. Equivalent circuit analysis shows good agreement with experimental results.

I. Introduction

The heterojunction bipolar phototransistors (HPTs) in three-terminal (3T) configuration are of great interest because of their potential as high performance photodetectors and as a possible alternative to a PIN/FET combination in radio over fibre communication systems, Suematsu and Imai[1].

The 3T-HPTs have a structure similar to that of the heterojunction bipolar transistor (HBT) with a window area on its emitter side for the optical input and can keep the excellent RF performances of the HBTs. Recently, 3T-HPTs with an unit optical gain cut-off frequency f_c higher than 10 GHz have been achieved, Fukano[2], Kamitsuma et al[3], Gonzalez et al[4]. The HPT detects the incident photons in the base and collector layers and amplifies the photocurrent through the transistor gain mechanism. The gain of the photocurrent is electrical. Consequently, the unit current gain cut-off frequency f_t of the HPT sets the upper limit for the value of the f_c, for a given layer structure Barros et al[5]. The difference between the f_t and f_c values, measured experimentally is usually large [2,3]. In this paper, we propose an improved base contact design in order to minimise this difference and to optimise the frequency performance of the HPTs.

II- Fabrication and Design of HBT phototransistors (HPTs)

II.A - Layer structure

The HPT structures are grown by Chemical Beam Epitaxy (CBE) on 2'' iron doped semi-insulating InP substrate. The layer structure is described in Table 1. $SiBr_4$ and CBr_4 are the sources used for n- and the p-type doping, respectively Benchimol et al[6]. The advantage of the CBE technique for the growth of such structure is its capability to control high p-type carbon doping (up to 10^{20} cm^{-3}) in $In_{0.53}Ga_{0.47}As$. The base layer thickness can thus be precisely controlled, without the need of $In_{0.53}Ga_{0.47}As$ undoped spacer as is necessary for diffusive dopants (Be or Zn). Moreover, unlike Metal Organic Chemical Vapour Deposition (MOCVD) technique, the etching effects induced by Bromine are minimised because of the high efficiency of the CBr_4 source, and there is no passivation effect of Carbon in $In_{0.53}Ga_{0.47}As$ related to the presence of Hydrogen.

II.B- Device Fabrication

HPTs are fabricated using a three-mesa technology to make contact with the emitter, base and collector layers. The emitter mesa is chemically etched, the base mesa is obtained through a combination of ion beam and wet etching, the latter in order to prevent base-collector leakage related to the etching process. Phototransistor insulation is performed by wet etching. For selective wet etching, the etching mixtures are $H_3PO_4/H_2O_2/H_2O$ for $In_{0.53}Ga_{0.47}As$, and H_3PO_4/HCl for InP. The n- and p- ohmic contacts are realised with Ti(500 Å)/Au(2500 Å), and annealed at 300°C under Nitrogen flux. Contact resistivities of 5.10^{-7} $\Omega.cm^{-2}$ and 10^{-5} $\Omega.cm^{-2}$ were obtained for the n- and p- ohmic contact, respectively, and the sheet base resistance was around 500 Ω/square. Finally, polyimide film is used for planarisation and isolation, and no antireflection coating is added.

II.C- Base contact definition

InP/InGaAs HBT phototransistors use the HBT configuration developed in our laboratory. For this configuration, the metallic base contact surrounds the emitter mesa. In order to realise the optical window for topside illumination, we suppress a part of this base contact, and so the light is directly incident on the base layer. In this work, two types of structures were realised according to the base contact design as shown in Figure 1. For the type A HPT, the metallic base contact surrounds three of the four edges of the emitter, as for the type B HPT, the base contact is only on one side of the emitter, opposite to the optical window. Both type A and type B HPTs have the same emitter area equals to 16 µm² with a base-collector junction equals to 216 and 162 µm², respectively. The optical window for the type-A is 88 µm², and for the type-B is 56 µm². The purpose of those two HPT configurations is to show the dependence of the HPT frequency performance versus the base contact design.

III. Results and Modelling

Both electrical and optical measurements were made on each type of phototransistor by using an on-wafer probe station.

III.A- Electrical characteristics of the HPTs

At first, we investigated the HPT in the electrical domain. The electrical characteristics were obtained without illumination and the S-parameters were measured with a network analyser ranging from 250 MHz to 65 GHz. The frequency dependence of the current gain H_{21} and the Mason's unilateral power gain G_{max} were calculated from the S-parameters. Both H_{21} and G_{max} are dependent on the collector current Ic and the best performances were achieved at the emitter-collector voltage Vce = 1.6 V, base current Ib = 345 µA and collector current Ic = 6 mA. Bias conditions for the two types of HPTs were the same. From H_{21} and G_{max} curves shown in Figure 2, we estimated the unit current gain cut-off frequency f_T and the maximum oscillation frequency f_{max}. These values (summarised in the Table 2a, are 60 GHz (f_T) and 35 GHz (f_{max}) for type A and 55 GHz (f_T) and 18 GHz (f_{max}) for type B.

In the Table 2, we dissociated the embedded (2a) and the de-embedded (2b) performances, because the test environment wafer influences the dynamic performances of the HPT. In fact, the access and the transmission lines induce some loss not included during the calibration of the s-parameters and photoresponse measurements. The parasitic parameters were determined by measuring an open and a short-circuit test structures placed on the same HPT wafer.

The relatively low values for f_T were mainly due to the large area of the base mesa necessary to the optical window. Moreover, type-A f_{max} is higher than type-B f_{max}., which can be explained by considering the base contact design for each HPT type. The metallic base contact encircles the three-quarter of the emitter mesa in type-A and the base resistance Rb decreases, compared to that of type-B. As f_{max} is approximately equals to $[f_T / 8\pi C_{bc} R_b]^{0.5}$, a lower value of the base resistance induces a higher f_{max}.

III.B- Optical characteristics of the HPTs

Next, HPTs were investigated as a photodetector using a HP8703 lightwave component analyser at the wavelength 1550 nm. The intensity of the light was modulated by a RF signal ranging from 130 MHz to 20 GHz. The light coupling was provided via a Cascade Microtech lightwave probe with a lensed single mode fibre with an illumination spot size equals to 5 µm. The frequency photoresponse of the two types of HPT was obtained under two bias conditions. One was the photodiode mode operation (PD-mode) with Vce = 1.6 V and Vbe = 0 V (without transistor effect) and the other one was the transistor mode operation (Tr-mode) with Vce equals to 1.6 V and Vbe > 0 V (with transistor effect).

The best optical characteristics were obtained in the same bias conditions as that used for electrical characterisation, i.e. Vce = 1.6 V and Ic = 6 mA. However, in optical characterisation the base current is the addition of two terms : the base current due to the injected electrical current and the base current due the photogenerated carriers. The total base current was 345 µA. This value was obtained for type-A with an average optical power equals to 700 µW and an electrical I_b = 160 µA, and for type-B with the same average optical power and an electrical I_b = 30 µA. The modulation index of the modulated optical power was 0.5.

Figure 3 shows the frequency photoresponse (R) of the two types of HPT. The photoresponse is expressed in dB, i.e. $R(dB) = 20.\log_{10}[\Re]$, where $\Re$ is the responsivity in A/W. The optical gain, G_{opt}, is defined as the difference between the Tr-mode photoresponse and the PD-mode photoresponse at low frequency. frequency for which the (extrapolated) Tr-mode photoresponse is equal to the DC PD-mode phoresponse (Fig. 3). Also, the unity optical gain cut-off frequency f_c is defined as the frequency for which the (extrapolated) Tr-mode gain is equal to the DC PD-mode gain (Fig. 3). The values of f_c estimated for the type-A and the type-B were 35 GHz and 42 GHz, respectively. All these results are summarised in the Table 2a. The optical performances, G_{opt} and f_c of the HPTs were lower than the electrical performances H_{21} and f_c.

The external DC responsivity, $\Re_{DC}$, of the type A and type B HPTs evaluated under the photodiode mode operation, were 0.29 A/W and 0.33 A/W, respectively.

III.C - Equivalent circuit analysis

A small-signal equivalent circuit model was developed for the fabricated HPTs. For electrical modeling, the phototransistor was characterized as an HBT with bias conditions similarly to those used for HPT. Under these bias conditions the S-parameters of the HPT with and without CW illumination are identicals. That means that the average optical power bias the base terminal as an electrical current and that the optical performances of the HPT is limited by its electrical performances.

Figure 4 shows the small-signal equivalent circuit model used for simulating the electrical behaviour of the HPTs. This equivalent circuit consists in an intrinsic HBT surrounded by a shell of parasitics. We used the T-representation to model the intrinsic device. Two base-collector capacitances C_{bcin} and C_{bcex} which correspond to the internal and external capacitances and a base-spreading resistances (R_{bex} and R_{bin}) were indispensable for simulating the S-parameters. C_{pbc}, C_{pbe}, C_{pce}, L_b, L_c, L_e are the parasitic elements associated to collector, emitter and base terminals and were evaluated from measurements of test structures placed on the same HPT wafer. The on-wafer S-parameters measurements were transformed into Y- and Z- parameters to subtract these parasitic effects.

Phototransistor equivalent circuit was obtained by adding to the HBT T-model a photocurrent source I_{ph} parallel to the base-collector capacitance, C_{bcph}, as shown in Figure 5. In this case, the parasitic elements are only those associated to collector and emitter terminals. The agreement between the measured and model-produced data was excellent over the frequency range of 130 MHz and 20 GHz. Table 3 summarises all the HPT parameters determinated in order to achieve the best fit between modelled and experimental data. Measured and simulated optical gain of HPT types A and B are shown in Figures 6 and 7.

IV. Discussion

We established in section III, that optical performances of HPT are limited by its electrical performances, i.e., that H_{21} and f_t set the upper limit for G_{opt} and f_c. Figure 8 and 9 show the frequency dependence of the current gain and optical gain for the two types of HPT. For type B, the optical gain curve is nearly equals to the current gain curve and the f_c to f_t ratio is 0.76. On the other hand, for type A structure the difference between G_{opt} and H_{21} is large and the f_c/f_t ratio is 0.58. We can explain these characteristics as follows. Under illumination, electron-hole pairs are created in the base and collector regions of the HPT. The photogenerated electrons are swept toward the subcollector and the photogenerated holes toward the base. The photoholes reaching the emitter region accumulate at the emitter/base junction and modify the potential barrier which causes a large electron current from emitter to collector. But not all the photogenerated holes reach the emitter area. In type A HPT, a large quantity of photoholes diffusing in the base under metallic contact will be eliminated via the base contact given rise to a high « leak » current. This component of photogenerated holes does not contribute to the optical gain. The high « leak » current measured at the base terminal can be associated to a lower base resistance. In contrast, type-B HPT offers a higher base resistance to the photogenerated holes diffusing under the base contact because, in this case, the base contact is placed behind the emitter region, opposite to the optical window. This base contact configuration allows a more efficient collection of photoholes at the emitter area resulting in a higher optical gain and an improved f_c/f_t ratio.

HPT equivalent circuit model simulates very well the photoresponse behaviour of both A and B types. Simulations show that the role of the base-spreading resistances, R_{bex} and R_{bin}, are very important for photoresponse performances. Estimated values of $R_b = R_{bex} + 2R_{bin}$, for A and B types were 42 Ω and 190 Ω, respectively. These values are in good agreement with experimental data.

However, the higher R_b leads to a lower f_{max} for type B HPT, as indicated in section III.A Therefore a trade-off between R_b and f_{max} is necessary to get according to the application of HPTs (photodetection, optoelectronic mixing, etc).

VI. Conclusion

We have reported the dependence of the 3T-HPT photoresponse characteristics according to the base contact configuration. We have shown that by realising an appropriated base contact design, the overall performance of the phototransistor can be improved with G_{opt} and f_c values near to the H_{21} and f_t upper limit values. Specifically, for type-B HPT we obtained a f_c = 42 GHz for a f_t = 55 GHz. This InP/InGaAs HPT offers the highest f_c/f_t = 0.76, yet reported.

***Acknowledgements*:** The authors would like to thank P. Berdaguer and A.M. Duchenois for assistance with device fabrication, C. Palma for modelisation work and A. Scavennec, C. Rumelhard and N. Chennafi for their valuable discussions. This work was partially supported by the ACTS/FRANS European project.

References

[1] E.Suematsu and N.Imai, «A fibre optic/millimetre-wave radio transmission link using HBT as direct photodetector and an optoelectronic up-converter », *IEEE Trans. Microwave Theory Tech., 1996, vol. 44, pp.133-143.*

[2] H. Fukano, « High-speed InP-InGaAs heterojunction phototransistors employing a nonalloyed electrode metal as a reflector », *IEEE J. Quantum Elect., 1994, vol.30, pp. 2889-2895.*

[3] H. Kamitsuna, Y. Matsuoka, S. Yamahata and K. Kurishima, « A monolithically integrated photoreceiver realized by InP/InGaAs double-heterostructure bipolar transistor technologies for optical/microwave interaction systems », *GaAs IC Symposium'95, pp. 185-188.*

[4] C.Gonzalez, C.Palma, J.Thuret, J.L.Benchimol, M.Riet, « InP/InGaAs HBT phototransistor as optoelectronic converter up to millimetre-wave bands », *MWP'97, Post-deadline Techn. Digest, Duisburg/Essen, 1997, pp. 9-12.*

[5] L. Barros, A. Paolella, M. Frankel, M. Romero, P. Herczfeld, and A. Madjar, « Photoresponse of microwave transistor to high-frequency modulated lightwave carrier signal », *IEEE Trans. MTT, 1997,vol.45, pp. 1368-1374.*

[6] J.L. Benchimol, J. MBA, A.M. Duchenois, B. Sermage, P. Launay, D. Caffin, M. Meghelli, M. Juhel, « CBE growth of Carbon doped InGaAs/InP HBTs 25 Gbit/s circuits », *J. Crystal Growth, 1998, vol.188, pp.349.*

Device layer:	Material :	Doping : (atm/cm^3)	Thickness (Å)
Emitter contact	InGaAs : n^+ InP : n^+	Si : 2.10^{19} Si : 2.10^{19}	1000 500
Emitter	InP : n	Si : 2.10^{17}	1000
Base	InGaAs : p^+	C :$2.5.10^{19}$	600
Collector	InGaAs : n	Si : 2.10^{16}	5500
Subcollector	InGaAs : n^+ InP : n^+	Si :2.10^{19} Si :$1.5.10^{19}$	2000 3000
Substrate	InP : SI	Fe	450 µm

Table 1 : HPT epitaxial layer parameters.

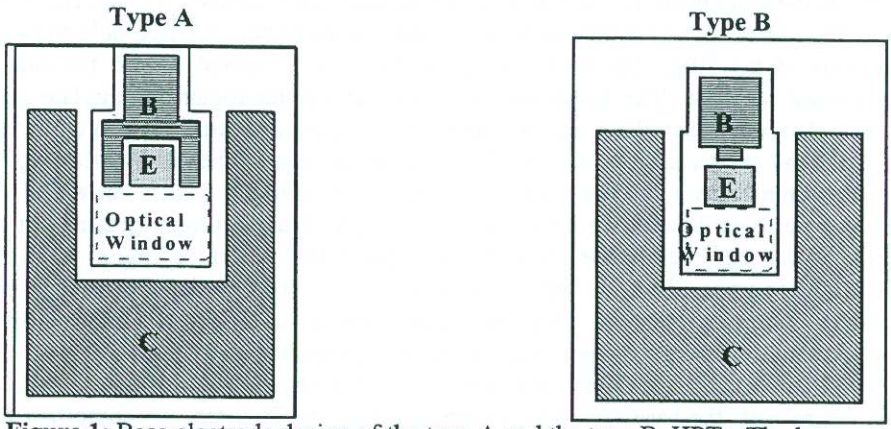

Figure 1: Base electrode design of the type A and the type B HPTs. The letters B, E and C correspond to the Base, Emitter and Collector contacts, respectively.

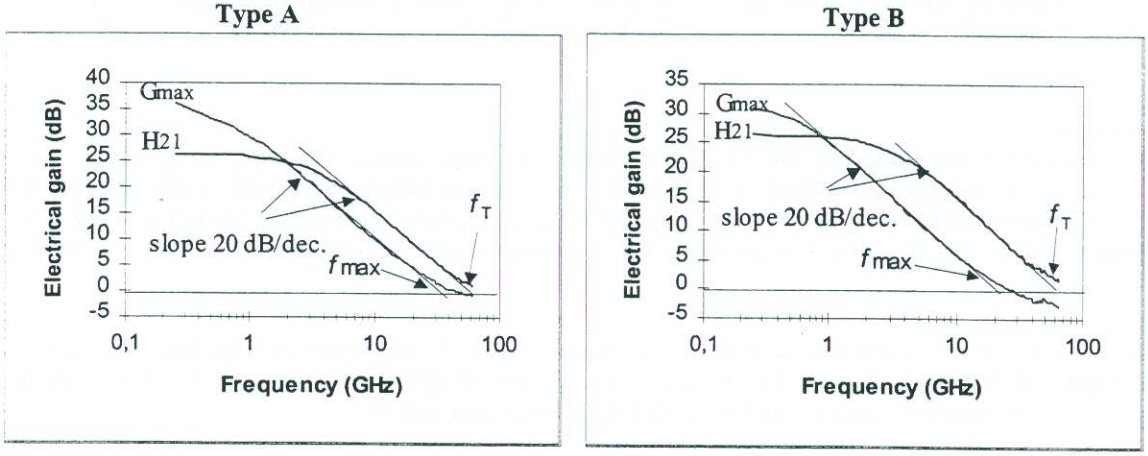

Figure 2: Current gain H_{21} and the Mason's unilateral power gain G_{max} of both A and B HPT types. The bias conditions are Vce=1.6 V, Ic=6 mA and Ib=345 µA, for the two types of HPT.

	(a)					(b)				
	Embedded performance					De-embedded performance				
	Electrical Charac.			Optical Charac.		Electrical Charac.			Optical Charac.	
HPT	H_{21}* dB	F_T GHz	F_{max} GHz	G_{opt}*dB	F_c GHz	H_{21}* dB	F_T GHz	F_{max} GHz	G_{opt}*dB	F_c GHz
type A	26	60	35	17	35	26	62	38	17	36
type B	26	55	18	24	42	26	60	20	24	44

Table 2 : Values of H_{21}, f_t, f_{max}, for the two types HPTs. The embedded (a) and de-embedded (b) values correspond to the HPT characteristics with and without measurement parasites, respectively. *H_{21} and G_{opt} values are measures given at 250 MHz and 130 MHz, respectively.

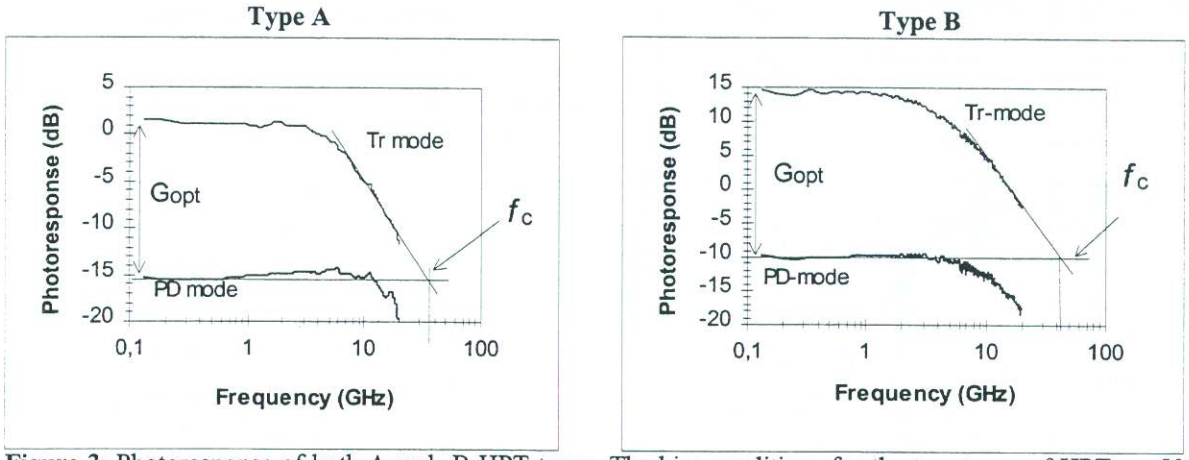

Figure 3: Photoresponse of both A and B HPT types. The bias conditions for the two types of HPT are Vce=1.6 V, Ic=6 mA and P_{avg}=700 µW with the modulation index m equals to 0.5.

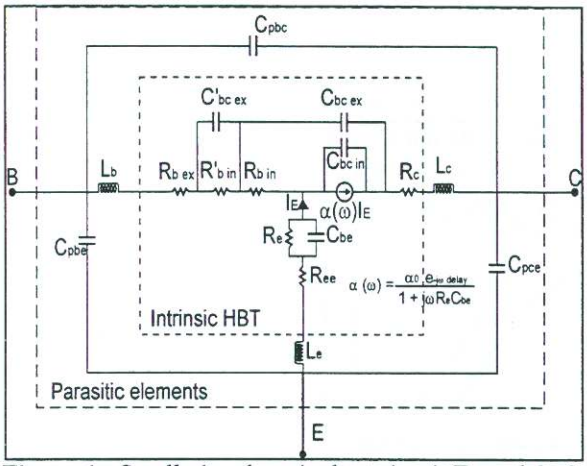

Figure 4 : Small-signal equivalent circuit T-model of the HBT part of HPT.

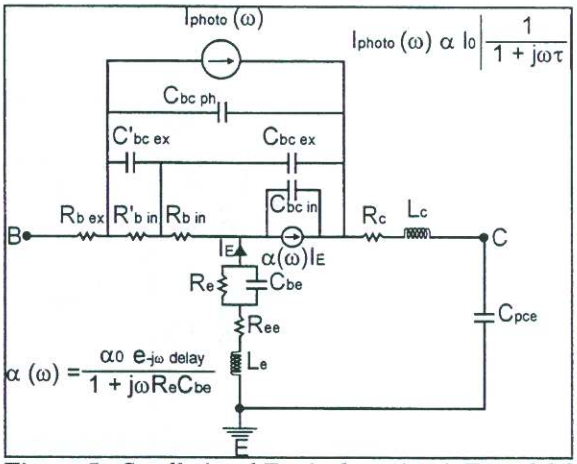

Figure 5 : Small-signal Equivalent circuit T-model for the Tr-mode operation of HPT.

HPT Type :	A	B
Parameters :	**Values :**	
P_{avg}	700 µW	700 µW
$C_{bc,ph}$	80 fF	110 fF
I_0	192.5 µA	805 µA
τ	4 ps	5.5 ps
R_e	5 Ω	5.5 Ω
R_{ee}	7.8 Ω	5 Ω
R_{bex}	8 Ω	30 Ω
$R_{bin1,2}$	17 Ω	80 Ω
R_c	10 Ω	15 Ω
$C_{bcex1,2}$	30-25 fF	26-20 fF
C_{bcin}	30 fF	21 fF
C_{be}	40 fF	40 fF
α_0	0.954	0.956
delay	1 ps	1.4 ps
Measurement parasites		
L_e	40 nH	
L_b, L_c	30 nH	
C_{pbc}	10 fF	
C_{pbe}, C_{pce}	20 fF	

Table 3 : Estimated parameters values in the small-signal T-model concerning the Tr-mode operation of HPT. The bias conditions were the same for the two types of HPT.

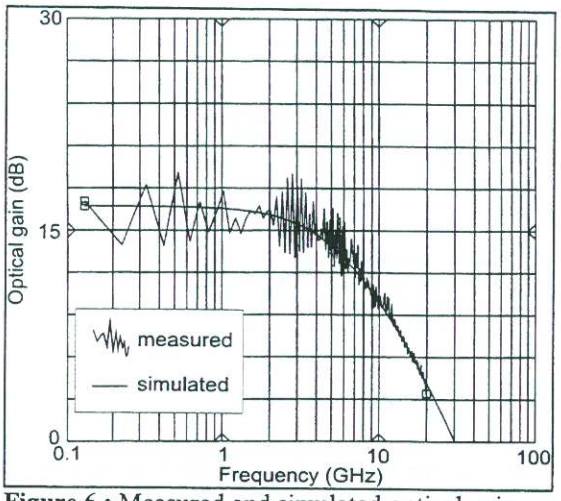

Figure 6 : Measured and simulated optical gain of HPT typeA.

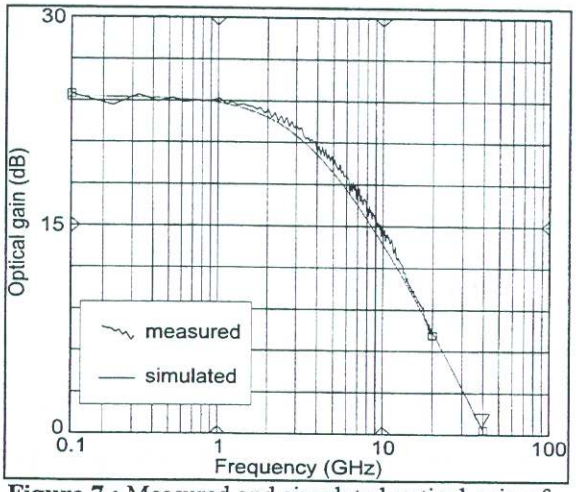

Figure 7 : Measured and simulated optical gain of HPT type B.

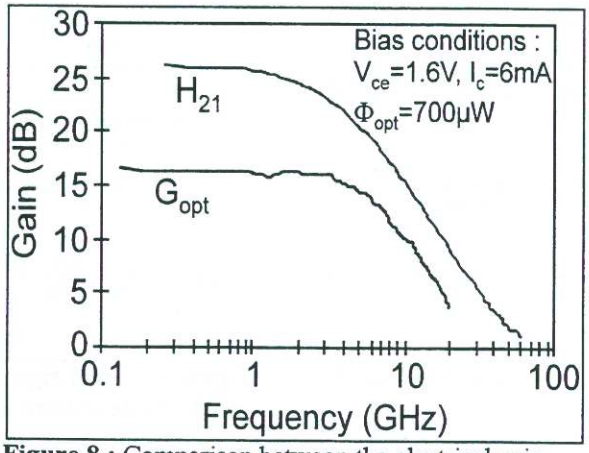

Figure 8 : Comparison between the electrical gain and the optical gain for HPT type A.

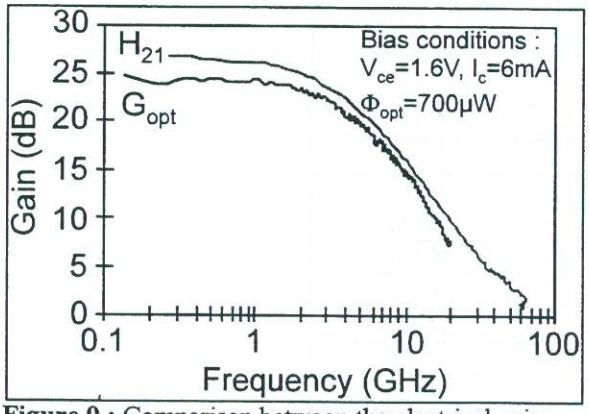

Figure 9 : Comparison between the electrical gain and the optical gain for HPT type B.